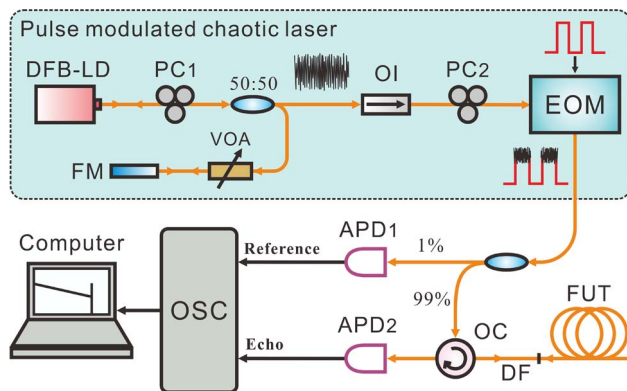


Combined Attenuation and High-Resolution Fault Measurements Using Chaos-OTDR

Volume 7, Number 6, December 2015

Xiangyu Dong
Anbang Wang
Jianguo Zhang
Hong Han
Tong Zhao
Xianglian Liu
Yuncaai Wang



DOI: 10.1109/JPHOT.2015.2501650
1943-0655 © 2015 IEEE

Combined Attenuation and High-Resolution Fault Measurements Using Chaos-OTDR

Xiangyu Dong,^{1,2} Anbang Wang,^{1,2} Jianguo Zhang,^{1,2} Hong Han,^{1,2}
Tong Zhao,^{1,2} Xianglian Liu,^{1,2} and Yuncai Wang¹

¹Key Laboratory of Advanced Transducers and Intelligent Control System, Ministry of Education and Shanxi Province, Taiyuan University of Technology, Taiyuan 030024, China

²Institute of Optoelectronic Engineering, College of Physics and Optoelectronics, Taiyuan University of Technology, Taiyuan 030024, China

DOI: 10.1109/JPHOT.2015.2501650

1943-0655 © 2015 IEEE. Translations and content mining are permitted for academic research only.

Personal use is also permitted, but republication/redistribution requires IEEE permission.

See http://www.ieee.org/publications_standards/publications/rights/index.html for more information.

Manuscript received September 30, 2015; revised November 4, 2015; accepted November 11, 2015. Date of publication November 8, 2015; date of current version December 2, 2015. This work was supported in part by the National Natural Science Foundation of China under Grant 61475111, Grant 61205142, and Grant 61227016; in part by the International Science and Technology Cooperation Program of China under Grant 2014DFA50870; in part by the Natural Science Foundation for Excellent Young Scientists of Shanxi Province under Grant 2015021004; in part by the Key Program for Shanxi Innovative Research Team for Science and Technology under Grant 2013091021; in part by the Program for the Innovative Talents of Higher Learning Institutions of Shanxi; and in part by the Program for Excellent Talents in Taiyuan University of Technology under Grant 2014YQ001. Corresponding authors: A. Wang and Y. Wang (e-mail: wanganbang@tyut.edu.cn; wangyc@tyut.edu.cn).

Abstract: We propose a combined attenuation and high-resolution fault measurement method using chaos optical time-domain reflectometry (OTDR). Utilizing the pulse-modulated chaotic light and correlation operation, this technique realizes fiber attenuation measurement and a distance-independent spatial resolution simultaneously. We demonstrate a proof-of-concept experiment for measurements of a single-mode fiber (G.652) and a fiber link consisting of a single-mode fiber (G.652) and a conventional (62.5- μm) multimode fiber. The measurement results show that different attenuation coefficients can be measured, and the coefficients agree well with the values obtained by using conventional OTDR. A 0.6-m resolution is achieved with a data acquisition bandwidth of 200 MHz.

Index Terms: Chaos, fiber attenuation, optical time domain reflectometry (OTDR).

1. Introduction

Conventional optical time domain reflectometry (OTDR) [1] is the most commonly used tool to characterize optical fibers. OTDR can locate and distinguish fiber faults such as breakpoints, mismatches, and bends by transmitting short optical pulses and analyzing the echo signals. The attenuation distribution along the fiber can be measured. However, the spatial resolution of the pulsed OTDR is typically only several meters. In particular, this technique suffers from a significant shortcoming: the tradeoff between dynamic range and spatial resolution. Many techniques have been proposed to eliminate this shortcoming. Ultrashort pulse techniques and optical low-coherence reflectometry were proposed to obtain a higher spatial resolution [2]–[5], but they are unsuitable for practical applications because of the requirement of complicated and expensive devices. Moreover, coding techniques [6]–[12] can enable larger measurement distances and

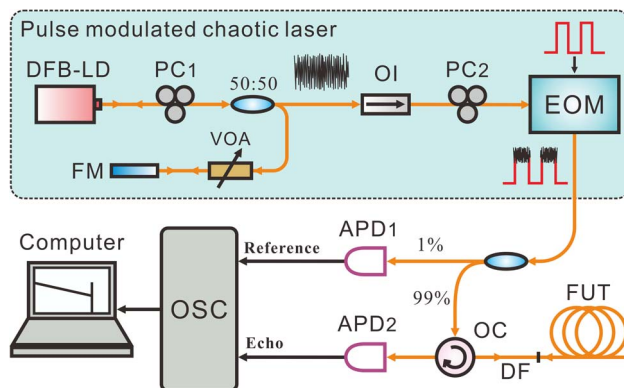


Fig. 1. Experimental setup of the proposed technique. DFB-LD: distributed-feedback laser diode; PC: polarization controller; VOA: variable optical attenuator; FM: fiber mirror; OI: optical isolator; EOM: electro-optical modulator; OC: optical circulator; DF: dummy fiber; FUT: fiber under test; APD: avalanche photodiode; OSC: oscilloscope.

obtain a spatial resolution of the unit pulse typically tens of meters, but the accuracy of measurement is still limited by the bandwidth of the codes.

Chaos optical time domain reflectometry (chaos-OTDR) [13] is a promising technique for fiber measurement. In this method, continuous-time chaotic laser light is employed as a probe light, which has a random intensity fluctuation and a delta-like autocorrelation trace. The correlation operation realizes fault location with a 6-cm distance-independent spatial resolution. Since then, other OTDR techniques based on chaotic light have been proposed [14]–[20]. For example, achievements of a 100-km measurement range [14] and sub-mm accuracy [15] have been reported. At present, the bandwidth of chaotic light generated by a semiconductor laser can easily reach several gigahertz and may be further enhanced up to more than 20 GHz [16], [17], which brings much higher resolution. Moreover, the chaos-OTDR can be applied to an optical passive network for fault detection [18]–[20]. However, currently, this technique can only be used to detect reflection events. As of now, fiber attenuation measurement by this method has not been reported.

In this paper, we propose an improved chaos-OTDR technique to realize the measurement of fiber attenuation. In this technique, a pulse modulated chaotic laser is used as a probe light. The distance-independent high spatial resolution is obtained by cross-correlation between the reference and echo signal. A proof-of-concept experiment is demonstrated. Experimental results indicate that different fiber attenuation coefficients can be measured, and they show good agreement with values obtained by a conventional OTDR. Furthermore, we achieved a 0.6-m spatial resolution under a 200-MHz data bandwidth.

2. Experiments

2.1. Experimental Setup

The experimental setup is shown in Fig. 1. The pulse modulated chaotic laser, as plotted in the dashed frame, serves as the probe light source. The continuous chaotic laser light is generated by a distributed-feedback laser diode (DFB-LD) with optical feedback. The laser with a 10.4-mA threshold current operates at 1549.6 nm. The operation temperature and operation wavelength of the laser are stabilized by a temperature controller. A 50:50 optical fiber coupler is used to split the emission of the laser into two branches: One works as the output and the other as the feedback. In the feedback path, the polarization and strength of the feedback light which comes from the reflection of a fiber mirror (FM) can be adjusted by a polarization controller (PC1) and a variable optical attenuator (VOA), respectively. An optical isolator (OI) is used to prevent unwanted feedback light. The electro-optic modulator (EOM) driven by a periodic-pulse signal generator is

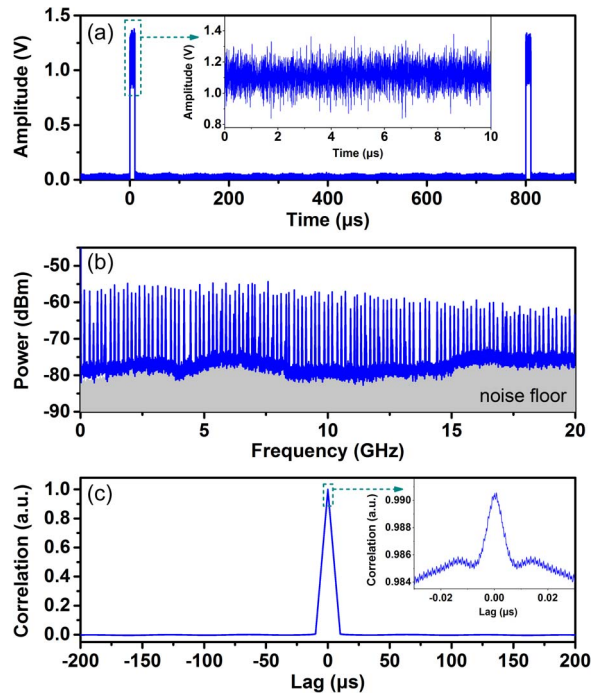


Fig. 2. Property of the probe signal. (a) Temporal waveform, (b) power spectrum, and (c) auto-correlation trace.

used to modulate the chaotic light. The polarization of the light injected into the EOM is adjusted by another polarization controller (PC2). The transmission light output from the EOM is divided by a 99:1 fiber coupler, where 99% and 1% of the input light serve as probe light and reference light, respectively.

When we measure a fiber link, the probe light is launched into the fiber under test (FUT) through an optical circulator (OC) and a dummy fiber (DF) which is used to calibrate the results and reduce the effect of the near-end reflection. The echo light induced by Rayleigh scattering and Fresnel reflections from the fiber is detected by a 200-MHz bandwidth avalanche photodiode (APD2). The reference light is detected by another identical avalanche photodiode (APD1). Then the reference and echo signal are all recorded by a real-time oscilloscope (OSC) with 1-GHz bandwidth and 5-GS/s sampling rate. Finally, the correlation and further processing are performed by a computer as indicated below. We note that, by considering bandwidth match with the APDs, a 200-MHz bandwidth of data acquisition and a 1-GS/s sampling rate is sufficient to achieve the same spatial resolution as the current experimental arrangement. Therefore, a data acquisition card or an application specific integrated circuit (ASIC) can be used to replace the oscilloscope used in this proof-of-concept experiment for the purpose of reducing system complexity and cost.

2.2. Experimental Results

Fig. 2 shows the properties of the probe signal. In Fig. 2(a), the waveform is plotted. The pulse width is 10 μs with an 800 μs signal period, which can be adjusted according to the detection range. The random trace at the top of the pulses is the chaotic signal and is enlarged in the inset. The periodic fluctuation on the bottom is caused by the APD. The power spectrum of the probe signal, plotted in Fig. 2(b), is measured by a spectrum analyzer via a 47-GHz photodetector. The envelope of this trace denotes the spectrum of the chaotic signal. Obviously, the chaotic signal has a wideband spectrum over 10-GHz bandwidth. Fig. 2(c) depicts the autocorrelation curve of one period of the probe signal. A thin and sharp peak which is caused by the chaotic signal is at

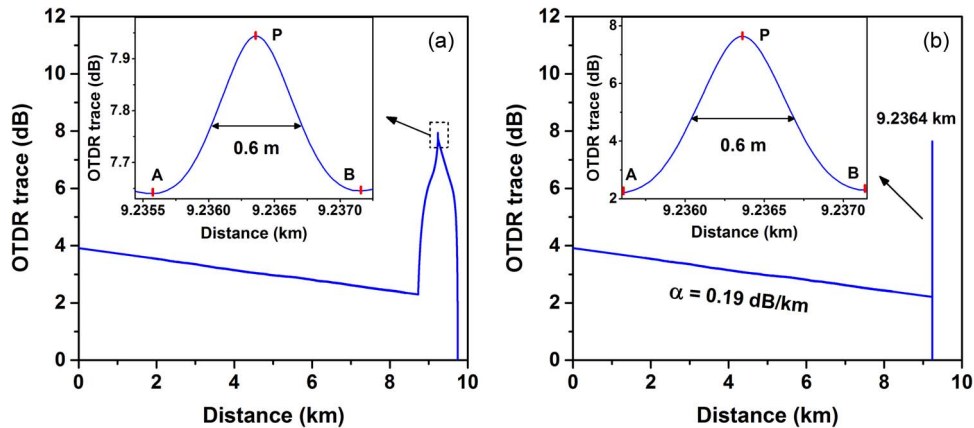


Fig. 3. Measurement results for a single mode fiber with a length of 9.2364 km. (a) Raw reflectometer trace directly obtained by calculating the echo signal and reference signal. (b) Optimized trace with peak fitting.

the top of the wide peak arising from the pulse. Limited by the 200-MHz bandwidth of the APD, the full-width-at-half-maximum (FWHM) of the narrow peak is about 6 ns.

The measurement results of a 9.2364-km long single mode fiber (G. 652) are shown in Fig. 3. The average power of the probe light is $56 \mu\text{W}$ and the pulse width is $5 \mu\text{s}$. Fig. 3(a) shows the raw reflectometer trace which is the semi-logarithmic correlation trace between the echo signal and the reference signal. In order to enhance signal-to-noise ratio, 500 correlation traces are averaged. This trace consists of two parts: an oblique line and a correlation peak. The oblique line is related to the fiber backscattering, and thus shows the fiber attenuation distribution. The line's slope represents the fiber attenuation coefficient. The correlation peak is actually the sum of the correlation between chaotic signals and the correlation between pulses. The former leads to the narrow apex marked in the dashed box, and the latter results in the wide lower part. The fault location is measured by the narrow apex that is the correlation peak of chaos, and the FWHM of this peak determines the spatial resolution of locating reflection events. We further optimize the raw reflectometer trace by eliminating the wide correlation peak caused by the pulse component. The method is Gaussian peak fitting because of that the correlation peak of chaos is similar to a Gaussian profile. First, we get the coordinate values of the correlation peak, i.e., the maximum point P shown in the inset of Fig. 3(a), and obtain the position of boundary points A and B which are the local minima located on each side of the peak. Second, by using these points and the FWHM value, a Gaussian peak is fitted to replace the original peak. The optimized curve is shown in Fig. 3(b), with the fitted peak plotted in the inset. In this figure, the measured attenuation coefficient of the fiber is 0.19 dB/km, which matches with the manufacturer product specification. The spike at the end of the trace with a 0.6-m spatial resolution represents the location of the fiber end. It is noted that the fiber attenuation in the range covered by the wide correlation peak cannot be measured accurately, even if the wide peak is eliminated with optimization. The length of this range is related to the pulse width and can be narrowed by reducing pulse width.

To demonstrate that the proposed OTDR can identify different attenuation coefficients, we measure two connected fibers with different attenuations. Specifically, a 5-km-long single mode fiber (G. 652) and a 5-km-long conventional ($62.5 \mu\text{m}$) multimode fiber are jointed with an optical fiber patchcord which is about 2-m long. Fig. 4(a) shows the OTDR trace measured by the proposed technique. As shown in this trace, the different attenuation coefficients of the fibers, insertion loss, and the reflection events can be detected. To verify these results, we also measure the same fiber link with a commercial single pulse OTDR (pulse width: 100 ns, measurement time: 3 minutes). The results of the two measurements agree well with each other, as shown in Fig. 4(b).

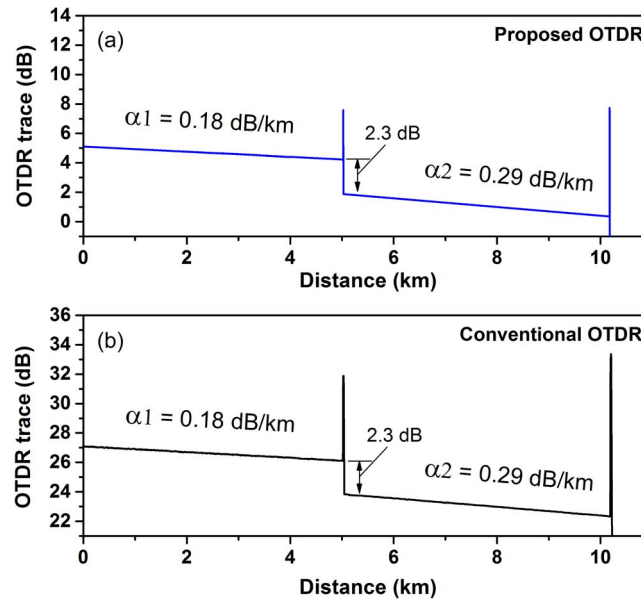


Fig. 4. OTDR trace of two connected optical fibers which have different attenuation coefficients measured by (a) the proposed OTDR and (b) a conventional OTDR.

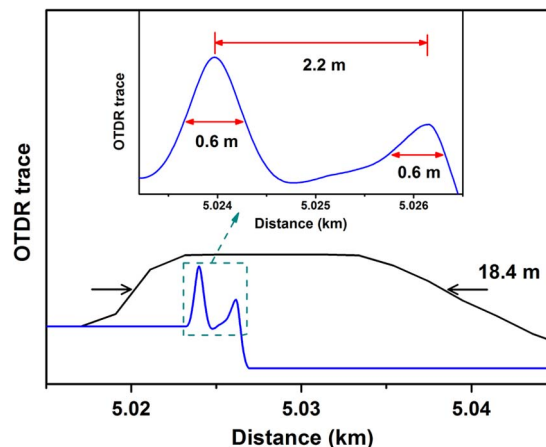


Fig. 5. Experimental detection results of two reflection events, which are measured by the proposed technique and conventional OTDR.

As mentioned previously, there is a patchcord between the two 5-km-long optical fibers in Fig. 4. We magnify the spikes induced by the connectors of the patchcord in Fig. 4(a) and (b) and compare the two magnified traces, as shown in Fig. 5. For the conventional OTDR, the measuring range is selected to be 20 km and the pulse width is set automatically as 100 ns. The spatial resolution of the black trace is 18.4 m, which is related to the pulse width, and the second connector cannot be detected. As shown by the blue trace which denotes the measurement result of the proposed technique, the two connectors can be detected and distinguished clearly. The spatial resolution of the proposed technique in this experiment is 0.6 m, as shown in the inset, and it is unrelated to the fiber length. It is worth noting that the spatial resolution is determined by the FWHM of the correlation peak which is inversely proportional to the signal bandwidth [19]. If we take advantage of the full bandwidth of the chaotic laser light, a spatial resolution of the order of microns can be achieved.

3. Conclusion

In summary, we propose and experimentally demonstrate an optical fiber diagnostic method. The fiber attenuation measurement is realized by using a pulse modulated chaotic laser. At the same time, this method retains a distance-independent high spatial resolution for reflection events. The proof-of-concept experiment shows that different fiber attenuations can be distinguished and the associated measurement results are highly consistent with the conventional OTDR. The 0.6-m spatial resolution is limited by the 200 MHz bandwidth of APDs in this experiment. The proposed method combines attenuation and fault measurement functions of Chaos-OTDR. We believe the proposed method is a promising solution for monitoring and precise fault location in fiber links.

Acknowledgment

The authors thank Prof. K. A. Shore and T. C. Scott for their helpful comments and suggestions. T. C. Scott is supported in China by the project GDW201400042 for the “high end foreign experts project.”

References

- [1] M. K. Barnoski and S. M. Jensen, “Fiber waveguides: A novel technique for investigating attenuation characteristics,” *Appl. Opt.*, vol. 15, no. 9, pp. 2112–2115, Sep. 1976.
- [2] S. Wielandy, M. Fishteyn, and B. Zhu, “Optical performance monitoring using nonlinear detection,” *J. Lightw. Technol.*, vol. 22, no. 3, pp. 784–793, Mar. 2004.
- [3] M. Legre, P. Thew, H. Zbinden, and N. Gisin, “High resolution optical time domain reflectometer based on 1.55 μm up-conversion photon-counting module,” *Opt. Exp.*, vol. 15, no. 13, pp. 8237–8242, Jun. 2007.
- [4] X. Clivaz, F. Marquis-Weible, and R. P. Salathe, “Optical low coherence reflectometry with 1.9 μm spatial resolution,” *Electron. Lett.*, vol. 28, no. 16, pp. 1553–1555, Jul. 1992.
- [5] K. Takada, A. Himeno, and K. Yukimatsu, “Resolution control of low-coherence optical time-domain reflectometer between 14 and 290 μm ,” *IEEE Photon. Technol. Lett.*, vol. 3, no. 7, pp. 676–678, Jul. 1991.
- [6] M. Nazarathy *et al.*, “Real-time long range complementary correlation optical time domain reflectometer,” *J. Lightw. Technol.*, vol. 7, no. 1, pp. 24–38, Jan. 1989.
- [7] K. Okada, K. Hashimoto, T. Shibata, and Y. Nagaki, “Optical cable fault location using correlation technique,” *Electron. Lett.*, vol. 16, no. 16, pp. 629–630, Jul. 1980.
- [8] M. Zoboli and P. Bassi, “High spatial resolution OTDR attenuation measurements by correlation technique,” *Appl. Opt.*, vol. 22, no. 23, pp. 3680–3681, Dec. 1983.
- [9] Y. Takushima and Y. C. Chung, “Optical reflectometry based on correlation detection and its application to the in-service monitoring of WDM passive optical network,” *Opt. Exp.*, vol. 15, no. 9, pp. 5318–5326, Apr. 2007.
- [10] M. Jones, “Using simplex codes to improve OTDR sensitivity,” *IEEE Photon. Technol. Lett.*, vol. 5, no. 7, pp. 822–824, Jul. 1993.
- [11] P. Healey, “Optical orthogonal pulse compression codes by hopping,” *Electron. Lett.*, vol. 17, no. 25, pp. 970–971, Dec. 1981.
- [12] D. Lee *et al.*, “SNR enhancement of OTDR using biorthogonal codes and generalized inverses,” *IEEE Photon. Technol. Lett.*, vol. 17, no. 1, pp. 163–165, Jan. 2005.
- [13] Y. Wang, B. Wang, and A. Wang, “Chaotic correlation optical time domain reflectometer utilizing laser diode,” *IEEE Photon. Technol. Lett.*, vol. 20, no. 19, pp. 1636–1638, Oct. 1, 2008.
- [14] Z. Wang *et al.*, “Long-range and high-precision correlation optical time-domain reflectometry utilizing an all-fiber chaotic source,” *Opt. Exp.*, vol. 23, no. 12, pp. 15514–15520, Jun. 2015.
- [15] Z. Xie *et al.*, “Fiber fault detection with high accuracy using chaotic signal from an SOA ring reflectometry,” *IEEE Photon. Technol. Lett.*, vol. 25, no. 8, pp. 709–712, Apr. 2013.
- [16] A. Uchida, T. Heil, Y. Liu, P. Davis, and T. Aida, “High-frequency broad-band signal generation using a semiconductor laser with a chaotic optical injection,” *IEEE J. Quantum Electron.*, vol. 39, no. 11, pp. 1462–1467, Nov. 2003.
- [17] A. Wang *et al.*, “Generation of flat-spectrum wideband chaos by fiber ring generator,” *Appl. Phys. Lett.*, vol. 102, no. 3, pp. 031112-1–031112-5, 2013.
- [18] L. Xia, D. Huang, J. Xu, and D. Liu, “Simultaneous and precise fault locating in WDM-PON by the generation of optical wideband chaos,” *Opt. Lett.*, vol. 38, no. 19, pp. 3762–3764, Oct. 2013.
- [19] A. Wang *et al.*, “Precise fault location in WDM-PON by utilizing wavelength tunable chaotic laser,” *J. Lightw. Technol.*, vol. 30, no. 21, pp. 3420–3426, Nov. 2012.
- [20] X. Dou *et al.*, “Experimental demonstration of the real-time online fault monitoring technique for chaos-based passive optical networks,” *Opt. Commun.*, vol. 350, no. 42, pp. 288–295, Sep. 2015.